This paper investigated post-fire thaw depth and its driving factors in East Siberian employing both field measurement and remote sensing proxies. Their findings indicate that: 1) fire exacerbates thaw depth, particularly when compared to unburned regions; 2) a combination of site moisture, forest composition, and fire severity accounts for 73.4% of thaw depth variability based on field investigations, while remote sensing proxies such as albedo, differenced Normalized Burn Ratio, land surface temperature, and NDVI contribute to explaining 66.3% of the variability.

The research explored topographical, vegetative, and burning effects on post-fire thaw depth in permafrost soil and mapped thaw depth with remote sensing data. Although the framework looks promising, some clarifications and elucidations are necessary to bolster more convincing findings. There are some limitations that I believe require further investigation.

We thank the reviewer for the constructive and valuable assessment of our paper. A point-by-point response is provided below. The original reviewer comments are in **bold**, *author comments in italic, and manuscript amendments are given in* green*.*

My major comments are:

1. **The manual selection process of driving factors for the MLR model appears insufficiently rigorous. Despite burn depth showing the highest correlation with thaw depth, it's omitted from the regression model. Do you have any thoughts on this selection?**

We thank the reviewer for pointing this out and we agree that the manual selection of the variables may have been somewhat subjective. Following your comment, we tested an automatic selection using a stepwise regression and we plan to include this revised regression in the revised manuscript.

We will adjust the '2.4 Statistical approach' section as follows:

2.4 Statistical approach

Our statistical analysis consisted of two major components. First, we assessed the environmental drivers of post-fire thaw depth using our field observations. Second, we evaluated how remote sensing variables can be used to predict field-measured thaw depth. For both analyses, we used an ordinary least squares (OLS) multiple linear regression (MLR) model with thaw depth as the response variable using the "statsmodels" Python module (Seabold and Perktold, 2010). We hypothesized that post-fire thaw depth relates to variables associated with topographic position (topographic position, site moisture, slope, and elevation), vegetation (stand age, basal area, vegetation density, and larch proportion), and fire severity (GeoCBI and burn depth). The selection of the environmental variables for the MLR model was based on a stepwise regression approach testing both forward selection and backward elimination. We calculated the relative importance of the retained variables to the MLR model explanatory power using the "pingouin" Python module (Vallat, 2018), which is based on the R package "relaimpo" (Grömping, 2006). The R^2 from the MLR model is partitioned by averaging over orderings among regressors using simple unweighted averages as proposed by Lindeman et al. (1980), providing a decomposition of the explained variance into non-negative contributions. Finally, we developed a MLR model using the remote sensing metrics (post-fire albedo, dNBR, LST, and pre-fire NDVI) as potential predictor variables to assess their capacity as proxies for post-fire thaw depth. The resultant obtained MLR was then spatially extrapolated to derive a continuous map of post-fire thaw depth over the study area.

In addition to these statistical analyses, which included all field plots, we also focused separately on two burned-unburned plot pairs. While our study area captured a large variability in landscape position, vegetation characteristics, and fire severity, these plots had the advantage of being spatially adjacent with a road acting as the fire barrier. Because of this, the landscape and

vegetation characteristics of these plots were very similar. As a result, these plot pairs represent interesting study cases in which the fire effect on thaw depth can be unequivocally separated from the landscape and vegetation influences.

The selection of the environmental variables based on the stepwise regression approach testing both forward selection and backward elimination resulted in the selection of the following variables: basal area, vegetation density and burn depth. Please find below the proposed new '3 Results' section:

3 Results

3.1 Environmental drivers of post-fire thaw depth

On average, summer thaw was deeper in burned (mean = 127.3 cm, standard deviation (sd) = 27.7 cm) than in unburned (98.1 cm, sd = 26.9 cm) plots (Fig. R1). An independent t-test indicated that this difference is statistically significant (p = 0.04). Thaw was deeper in uplands (Figs. R2, R3a, and R3d) and well-drained (Figs. R2 and R3b) landscape positions; in open (Figs. R2 and R4b), mature (R2 and R3e), and mixed forests which included tree species other than Cajander larch (Figs. R2 and R3f); and in high severity burns (Figs. R2, R3g, and R4c).

Based on the results of the stepwise regression, both forward selection and backward elimination, we retained basal area, vegetation density, and burn depth as predictor variables for the MLR (Fig. R4). The multiple linear regression results indicated that the selected environmental drivers together explained 73.3 % of the thaw depth variability. Burn depth was the main contributor for the MLR model explanatory power (Table R1).

3.2 Remote sensing proxies of thaw depth

Within the fire perimeter, there was considerable spatial variability in albedo, dNBR, LST, and pre-fire NDVI (Figs. R5 and R6). Albedo values inside the fire perimeter had a mean of 0.10 (sd = 0.02), compared to mean of 0.12 (sd = 0.02) outside the perimeter (Figs. R5a and R6a). The dNBR values from our 13 burned field plots ranged between 0.34 and 0.85, with a mean of 0.57, while for the entire fire perimeter the mean was 0.41 (sd = 0.27, Fig. R5b and R6b). In addition, LST values inside the fire scar were on average 5.24 K higher than the LST values outside the fire scar (Figs. R5c and R6c). However, for some parts of the fire scar, LST values exceeded the surrounding unburned pixels by approximately 20 K. For the pre-fire NDVI, the distributions of values inside and outside the fire perimeter were similar (Figs. R5d and R6d) with a mean NDVI value of 0.78 (sd = 0.08) inside the perimeter and and a mean NDVI value of 0.79 (sd = 0.07) outside the perimeter.

Thaw tended to be deeper in the plots with lower summer albedo (Fig. R7a), higher dNBR, (Fig. R7b), higher LST (Fig. R7c) and lower pre-fire NDVI (Fig. R7d). The correlation with LST was the strongest, while the correlations between thaw depth and dNBR, albedo and pre-fire NDVI were not statistically significant at $p < 0.05$ (Fig. R8).

Stepwise forward selection indicated that LST was the only variable to be selected for the linear regression, capturing 42.9 % of the variability in field-measured thaw depth. By contrast, stepwise backward elimination pointed dNBR, albedo, and pre-fire NDVI as the variables to be retained in the MLR model. Taken together, these three remote sensing proxies explained 66.3% of field-measured thaw depth variability. dNBR was the most important predictor in this model configuration (Table R2).

The MLR model for thaw depth based on dNBR, albedo, and pre-fire NDVI enabled spatially continuous thaw depth estimates over the study area, including uncertainty estimates (Fig. R9). We chose this MRL configuration due to the higher R^2, when compared to LST alone. Post-fire thaw depth varied largely within the fire scar, for example between 83.49 cm (5th percentile) and 226.42 cm (95th percentile), with a mean of 139.72 cm (sd = 43.76 cm). In contrast, for the pixels outside the fire perimeter, the estimated thaw depth varied between 66.59 cm (5th percentile) and 237.99 cm (95th percentile), with a mean of 125.08 cm

(sd = 52.15 cm) (Fig. R9c). On average, burned areas thus experienced 14.64 cm deeper summer thaw depth one year after the fire than unburned areas.

2. **Could you provide the significance for all the correlation matrices in Figures A1 and B1? Burn depth exhibits a positive correlation to thaw depth (0.53) and soil moisture (0.04), respectively, however, the thaw depth has a negative correlation (-0.53) to site moisture. This raises questions.**

We plan to add the significance of the correlations in the matrices in new figure versions of the revised manuscript. Below you can find these revised figures (Figs. R2 and R8).

Site moisture is a plot-level site moisture classification (Johnstone et al., 2008)*, defined as the "potential moisture available for plant growth". This classification assesses the site moisture based on local topographic drainage and also accounts for permafrost presence and soil texture. It results in a six-point scale (xeric, subxeric, subxeric to mesic, mesic, mesic to subhygric, and subhygric) ranging between dry and wet. As site moisture is a categorical variable, we ranked it on ordinal scale to include this variable in our linear analysis. Thus, when thaw depth shows a negative correlation with site moisture, that is indicative that drier (well-drained) plots tended to have deeper thaw. We will clarify this information in revision.*

2.2 Field data

[...]

We also assigned the topographic position of the plot in relation to its surroundings (upland, midslope, lowland) and plot-level site moisture classes following Johnstone et al. (2008). This approach assesses site moisture based on local topographic drainage thereby accounting for soil texture and permafrost presence. The resulting ordinal scale consists of six site moisture classes ranging between dry and wet (xeric, subxeric, subxeric to mesic, mesic, mesic to subhygric, and subhygric). The six classes represent the potential moisture availability for plant growth and should not be confused with temporally explicit soil moisture measurements. This site moisture classification has been used extensively in fire studies in boreal North America (Walker et al., 2020).

4 Discussion

4.1 Environmental drivers of post-fire thaw depth

[...]

Increasing fire severity tends to increase thaw depth (Alexander et al., 2018; Holloway et al., 2020; Jafarov et al., 2013; Jiang et al., 2015; Li et al., 2019). The positive correlations between the fire severity proxies burn depth and GeoCBI, and thaw depth found in our study is consistent with these previous results. In addition, fire severity is often influenced by vegetation and topographic conditions. In our study for example, the well-drained upland plots were characterized by deeper thaw , while lowland areas are usually wetter with limited drainage and shallow thaw (Figs. R2 and R3). These wet lowland ecosystems also tend to burn with lower severity (Benscoter et al., 2011; Dillon et al., 2011; Holloway et al., 2020; Turetsky et al., 2011).

3. **Regarding the application of multi-linear regression, are you utilizing the original data or standardized data? Expanding on this in section 2.4 Statistical Approach would enhance clarity.**

We used the original data. We will expand the statistical approach to include this information as suggested. A proposed new version of the '2.4 Statistical approach' section can be found in the answer to comment 1.

4. **Are the environmental factors and remote sensing proxies of thaw depth consistent between burned and unburned plots if you explore the data separately? How does the correlation coefficient fluctuate between burned and unburned regions?**

We acknowledge that our field dataset is somewhat limited in size. As a result, we feel that we cannot confidently infer any statistically relevant information by analyzing only 6 unburned plots. However, we would like to point out that the variables related to landscape position do not change in their definition between burned and unburned sites. The vegetation characteristics were based on a reconstruction of the pre-fire situation. Finally, for the fire severity measurements (namely burn depth and GeoCBI, where the unburned plots receive the values of 0) the correlation information when considering only the burned plots is shown in Fig. R10. When considering only burned plots, burn depth, the fire severity variable retained in the revised model, has a correlation coefficient of 0.55 with thaw depth, compared to 0.53 when all plots were analyzed.

5. **According to the MLR model, site moisture seems to play a more significant role in driving variations in thaw depth than fire severity. However, thaw depth in burned areas typically surpasses that of unburned areas on average. How do you consider the relative contributing importance of site moisture and burning severity? What are your thoughts on the potential driving mechanism of thaw depth by a comprehensive interpretation of the statistical model in this study? Furthermore, given the potential contribution of site moisture to thaw depth, why wasn't soil moisture remote sensing data considered?**

First, as showed in our answer to comment 1, with the revised stepwise selection of variables, site moisture is no longer retained in the MLR model. We appreciate the good suggestion of including the relative importance of the variables in the model. The inclusion of this metric is presented in the answer to comment 1. We have also discussed the relation between site moisture and fire severity in our answer to comment 2

Other small comments:

6. **Line 118: The reference for Johnstone et al. (2008) is missing.**

We thank the reviewer for the comment. However, we have checked and the reference is there in the list (line 528, in the first version of the manuscript).

Johnstone, J. F., Hollingsworth, T. N., and Chapin, F. S.: A key for predicting postfire successional trajectories in black spruce stands of interior Alaska., https://doi.org/10.2737/PNW-GTR-767, 2008.

7. **Line 234: Does the larch tree play a certain function in inducing boreal fires? What is the reason for retaining the larch proportion?**
8. **Lines 280 – 282: why do plots with fewer larch trees thaw deeper? You may expand some discussion here on larch proportion.**

Thanks for the comments, after the new selection of field variables, larch proportion is no longer retained in the MLR model. Regardless, we will expand this discussion about the role of larch trees on permafrost dynamics in the revised version of the manuscript.

Moreover, the presence of Cajander larch trees is closely coupled with permafrost (Herzschuh, 2020), as they maintain permafrost by controlling its seasonal thawing. In turn, the permafrost helps to provide sufficient water to the trees by preventing it from draining away quickly (Zhang et al., 2011). Our results reflect this vegetation-permafrost interaction, where plots with fewer larch trees showed a more pronounced thaw. Our observations in the field also revealed that larch trees were prevalent and tend to dominate in mesic and hygric parts of the landscape, including the lowlands with shallower permafrost thaw. Conversely, Scots pine was more prevalent in the drier upland areas, which showed deeper thaw (Fig. R2). Scots pine trees in the region are found on moderately warm and dry locations, for example on hilltops and well-drained summits of watersheds with sandy soils and deeper permafrost thaw. In contrast, larch trees are dominant in wide depressions with often cool waterlogged soils with shallower permafrost thaw (Isaev et al., 2010). Eastern Siberian larch trees are some of the only

tree species that can successfully grow on permafrost soils with very shallow thaw. This is due to their ability to develop the adventitious rooting system (Herzschuh, 2020; Kajimoto, 2010). Larch and also Scots pine have evolved under periodic fire conditions, with the capacity to regenerate and grow after fire (Kharuk et al., 2021). The competitive advantages have led to the establishment of larch dominance in Siberian permafrost environments. However, increasing permafrost degradation could lead to a shift in the dominant species, with larch being replaced by pine and other species (Zhang et al., 2011).

9. **Figures A1 & B1: please add significance to the correlation matrix.**

We will add significance to the correlation matrices as suggested (Figs. R2 and R8).

10. **Figures A2 & 3: For unburned areas where burn depth and GeoCBI are 0, it's worth showing what drives the thaw depth when there is no fire rather than explaining everything by one statistic model.**

Thanks for the comments. We have already addressed them in our response to comment 4.

11. **Line 405: please double-check all the references.**

Thanks for pointing this out, we have double-checked all references.

12. **Figure 4 (b) & (d): The fire scar wasn't fully covered.**
13. **Figure 8 (a) & (b): The fire scar wasn't fully covered.**

Unfortunately, there is no pre-fire image available that covers the northwestern tip of the fire scar. Figure 4b and d (in the first version of the manuscript) show that there is no data for that small portion. We will clarify this further in the caption (Fig. R5).

References

Alexander, H. D., Natali, S. M., Loranty, M. M., Ludwig, S. M., Spektor, V. V., Davydov, S., Zimov, N., Trujillo, I., and Mack, M. C.: Impacts of increased soil burn severity on larch forest regeneration on permafrost soils of far northeastern Siberia, For Ecol Manage, 417, 144–153, https://doi.org/10.1016/j.foreco.2018.03.008, 2018.

Benscoter, B. W., Thompson, D. K., Waddington, J. M., Flannigan, M. D., Wotton, B. M., De Groot, W. J., and Turetsky, M. R.: Interactive effects of vegetation, soil moisture and bulk density on depth of burning of thick organic soils, Int J Wildland Fire, 20, 418–429, https://doi.org/10.1071/WF08183, 2011.

Dillon, G. K., Holden, Z. A., Morgan, P., Crimmins, M. A., Heyerdahl, E. K., and Luce, C. H.: Both topography and climate affected forest and woodland burn severity in two regions of the western US, 1984 to 2006, Ecosphere, 2, https://doi.org/10.1890/ES11-00271.1, 2011.

Grömping, U.: Relative Importance for Linear Regression in R: The Package relaimpo, J Stat Softw, 17, https://doi.org/10.18637/jss.v017.i01, 2006.

Herzschuh, U.: Legacy of the Last Glacial on the present-day distribution of deciduous versus evergreen boreal forests, Global Ecology and Biogeography, 29, 198–206, https://doi.org/10.1111/geb.13018, 2020.

Holloway, J. E., Lewkowicz, A. G., Douglas, T. A., Li, X., Turetsky, M. R., Baltzer, J. L., and Jin, H.: Impact of wildfire on permafrost landscapes: A review of recent advances and future prospects, in: Permafrost and Periglacial Processes, 371–382, https://doi.org/10.1002/ppp.2048, 2020.

Isaev, A. P., Protopopov, A. V., Protopopova, V. V., Egorova, A. A., Timofeyev, P. A., Nikolaev, A. N., Shurduk, I. F., Lytkina, L. P., Ermakov, N. B., Nikitina, N. V., Efimova, A. P., Zakharova, V. I., Cherosov, M. M., Nikolin, E. G., Sosina, N. K., Troeva, E. I., Gogoleva, P. A., Kuznetsova, L. V., Pestryakov, B. N., Mironova, S. I., and Sleptsova, N. P.: Vegetation of Yakutia: Elements of Ecology and Plant Sociology, 143–260, https://doi.org/10.1007/978-90-481-3774-9_3, 2010.

Jafarov, E. E., Romanovsky, V. E., Genet, H., McGuire, A. D., and Marchenko, S. S.: The effects of fire on the thermal stability of permafrost in lowland and upland black spruce forests of interior Alaska in a changing climate, Environmental Research Letters, 8, https://doi.org/10.1088/1748-9326/8/3/035030, 2013.

Jiang, Y., Rocha, A. V., O'Donnell, J. A., Drysdale, J. A., Rastetter, E. B., Shaver, G. R., and Zhuang, Q.: Contrasting soil thermal responses to fire in Alaskan tundra and boreal forest, J Geophys Res Earth Surf, 120, 363–378, https://doi.org/10.1002/2014JF003180, 2015.

Johnstone, J. F., Hollingsworth, T. N., and Chapin, F. S.: A key for predicting postfire successional trajectories in black spruce stands of interior Alaska., https://doi.org/10.2737/PNW-GTR-767, 2008.

Kajimoto, T.: Root System Development of Larch Trees Growing on Siberian Permafrost, in: Permafrost Ecosystems, edited by: Osawa, A., Zyryanova, O., Matsuura, Y., Kajimoto, T., and Wein, R., Springer, Dordrecht, 303–330, https://doi.org/10.1007/978-1-4020-9693-8_16, 2010.

Kharuk, V. I., Ponomarev, E. I., Ivanova, G. A., Dvinskaya, M. L., Coogan, S. C. P., and Flannigan, M. D.: Wildfires in the Siberian taiga, Ambio, 50, 1953–1974, https://doi.org/10.1007/s13280-020-01490-x, 2021.

Li, X., Jin, H., He, R., Huang, Y., Wang, H., Luo, D., Jin, X., Lanzhi, L., Wang, L., Li, W., Wei, C., Chang, X., Yang, S., and Yu, S.: Effects of forest fires on the permafrost environment in the northern Da Xing'anling (Hinggan) mountains, Northeast China, Permafr Periglac Process, 30, 163–177, https://doi.org/10.1002/ppp.2001, 2019.

Lindeman, R. H., Merenda, P. F., and Gold, R. Z.: Introduction to Bivariate and Multivariate Analysis, Scott, Foresman, Glenview, IL, 1980.

Seabold, S. and Perktold, J.: Statsmodels: Econometric and Statistical Modeling with Python, in: Proceedings of the 9th Python in Science Conference, 92–96, https://doi.org/10.25080/Majora-92bf1922-011, 2010.

Turetsky, M. R., Donahue, W. F., and Benscoter, B. W.: Experimental drying intensifies burning and carbon losses in a northern peatland, Nat Commun, 2, https://doi.org/10.1038/ncomms1523, 2011.

Vallat, R.: Pingouin: statistics in Python, J Open Source Softw, 3, 1026, https://doi.org/10.21105/joss.01026, 2018.

Walker, X. J., Baltzer, J. L., Bourgeau-Chavez, L. L., Day, N. J., De groot, W. J., Dieleman, C., Hoy, E. E., Johnstone, J. F., Kane, E. S., Parisien, M. A., Potter, S., Rogers, B. M., Turetsky, M. R., Veraverbeke, S., Whitman, E., and Mack, M. C.: ABoVE: Synthesis of Burned and Unburned Forest Site Data, AK and Canada, 1983-2016, https://doi.org/10.3334/ORNLDAAC/1744, 2020.

Zhang, N., Yasunari, T., and Ohta, T.: Dynamics of the larch taiga-permafrost coupled system in Siberia under climate change, Environmental Research Letters, 6, https://doi.org/10.1088/1748-9326/6/2/024003, 2011.

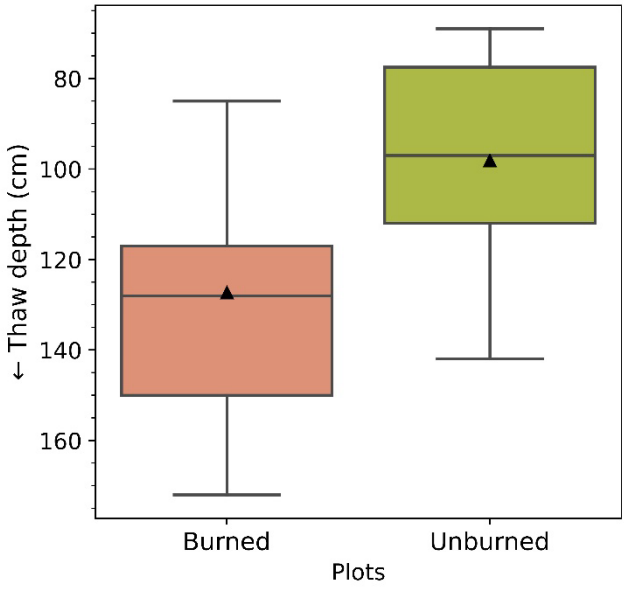

Figure R1: One year post-fire summer thaw was deeper in burned plots compared to unburned plots. Each box ranges from the first to the third quartile. Whiskers extend to points that lie within 1.5 times the interquartile range. The median is indicated by the horizontal line and the mean by the black triangle.

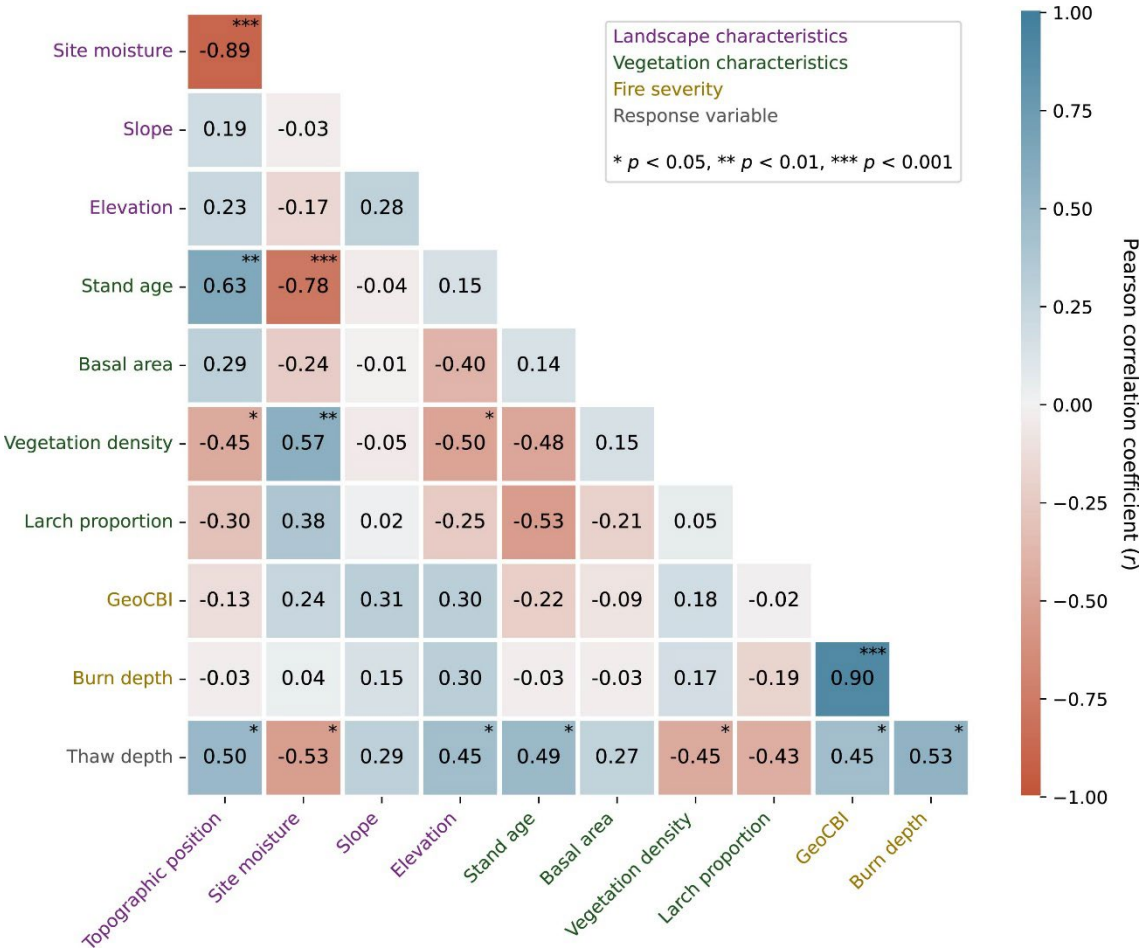

Figure R2: Correlation matrix between field-measured environmental variables representing landscape, vegetation and fire severity characteristics, and thaw depth. GeoCBI is the Geometrically structured Composite Burn Index.

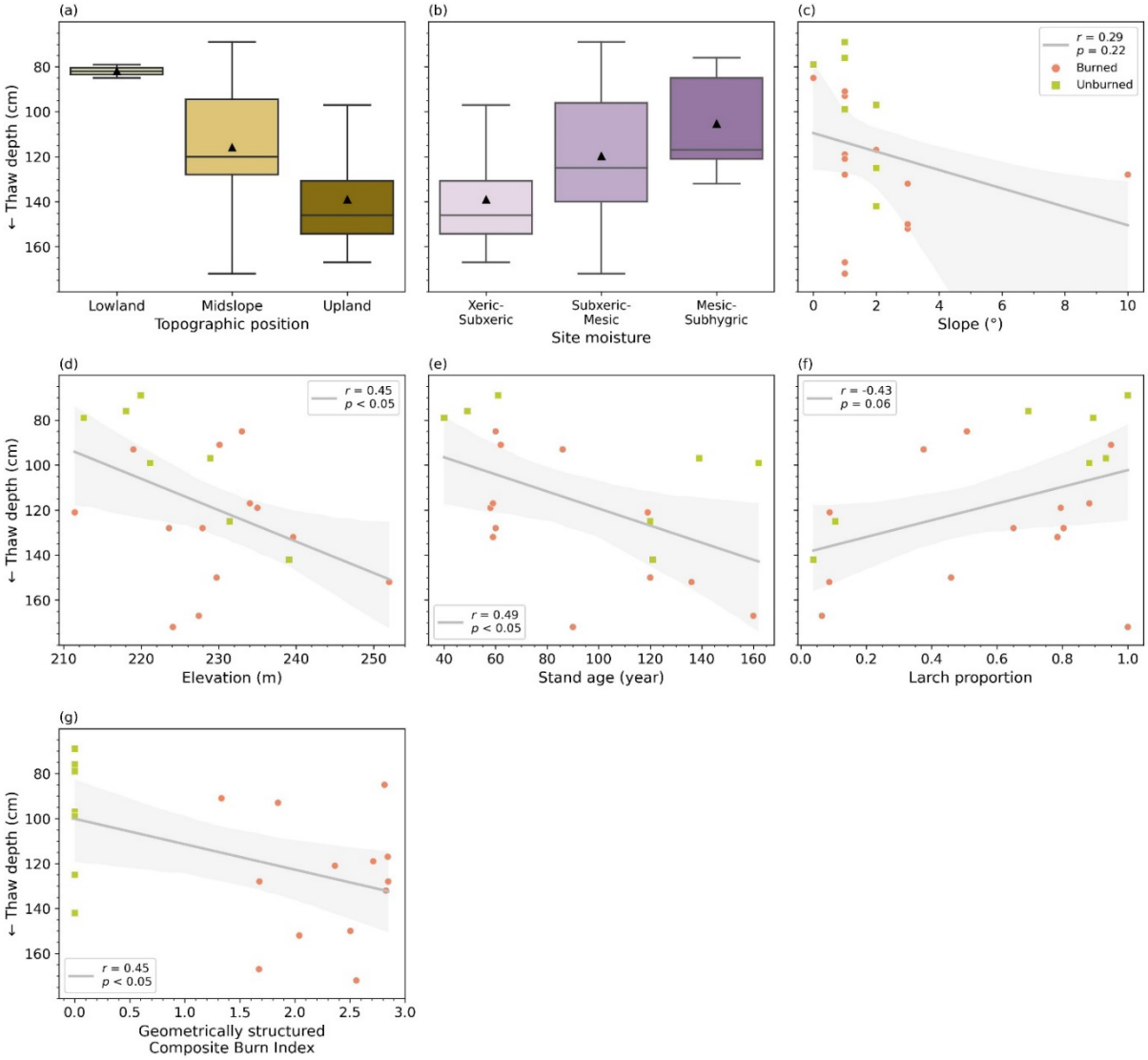

Figure R3: Relationships between (a) topographic position, (b) site moisture, (c) slope, (d) elevation, (e) stand age, (f) larch proportion, (g) Geometrically structured Composite Burn Index, and thaw depth. In (a) and (b), each box ranges from the first to the third quartile. Whiskers extend to points that lie within 1.5 times the interquartile range. The median is indicated by the horizontal line and the mean by the black triangle. For site moisture, classes were grouped together for better visualization.

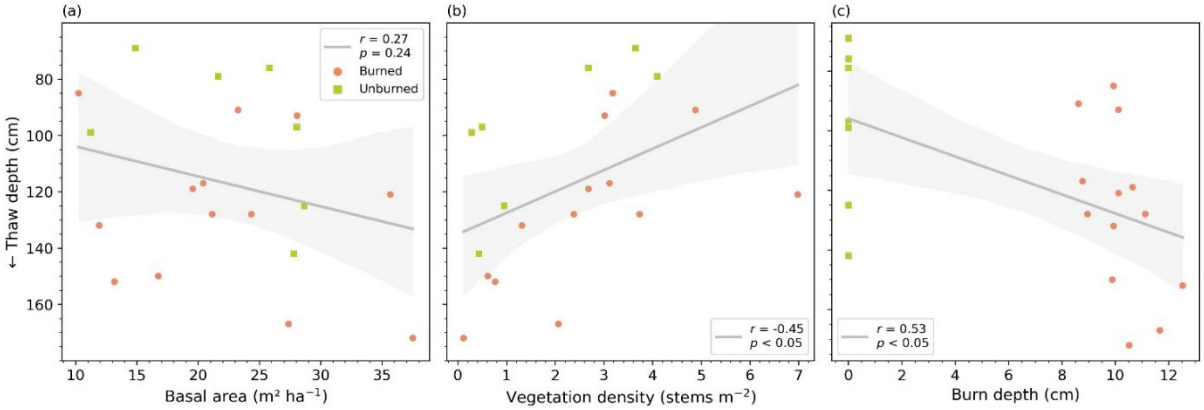

Figure R4: Relationships between field-measured thaw depth and (a) basal area, (b) vegetation density, and (c) burn depth.

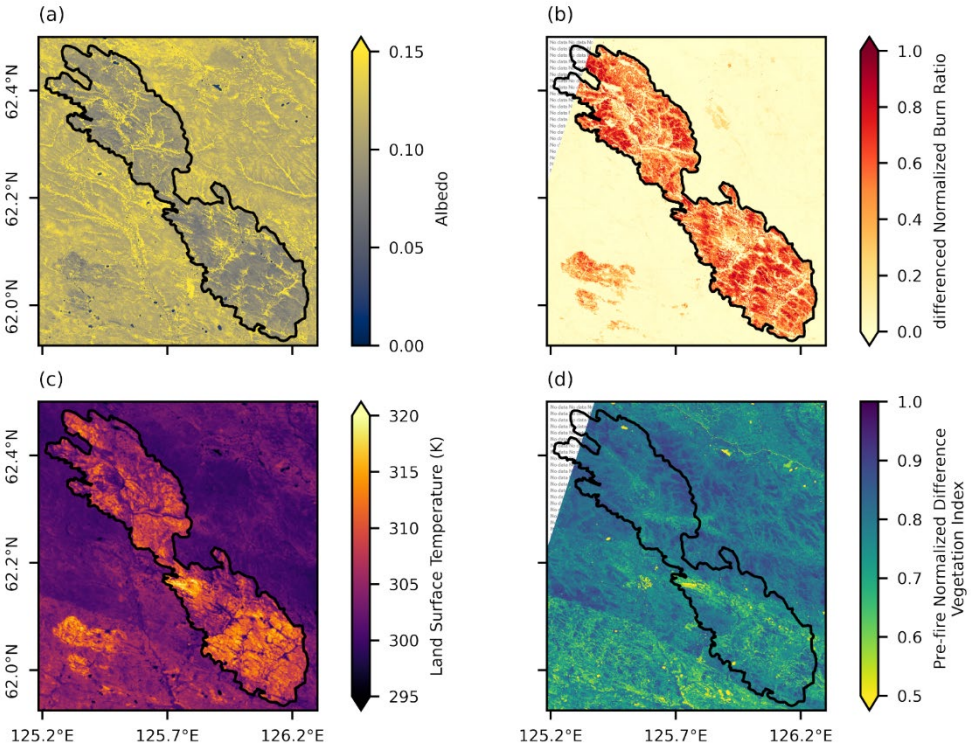

Figure R5: Maps showing (a) albedo, (b) differenced Normalized Burn Ratio, (c) land surface temperature, and (c) pre-fire Normalized Difference Vegetation Index derived from Landsat 8 imagery. In (b) and (c), the northwestern tip with "no data" indicates a portion that was not covered by the Landsat 8 pre-fire scenes.

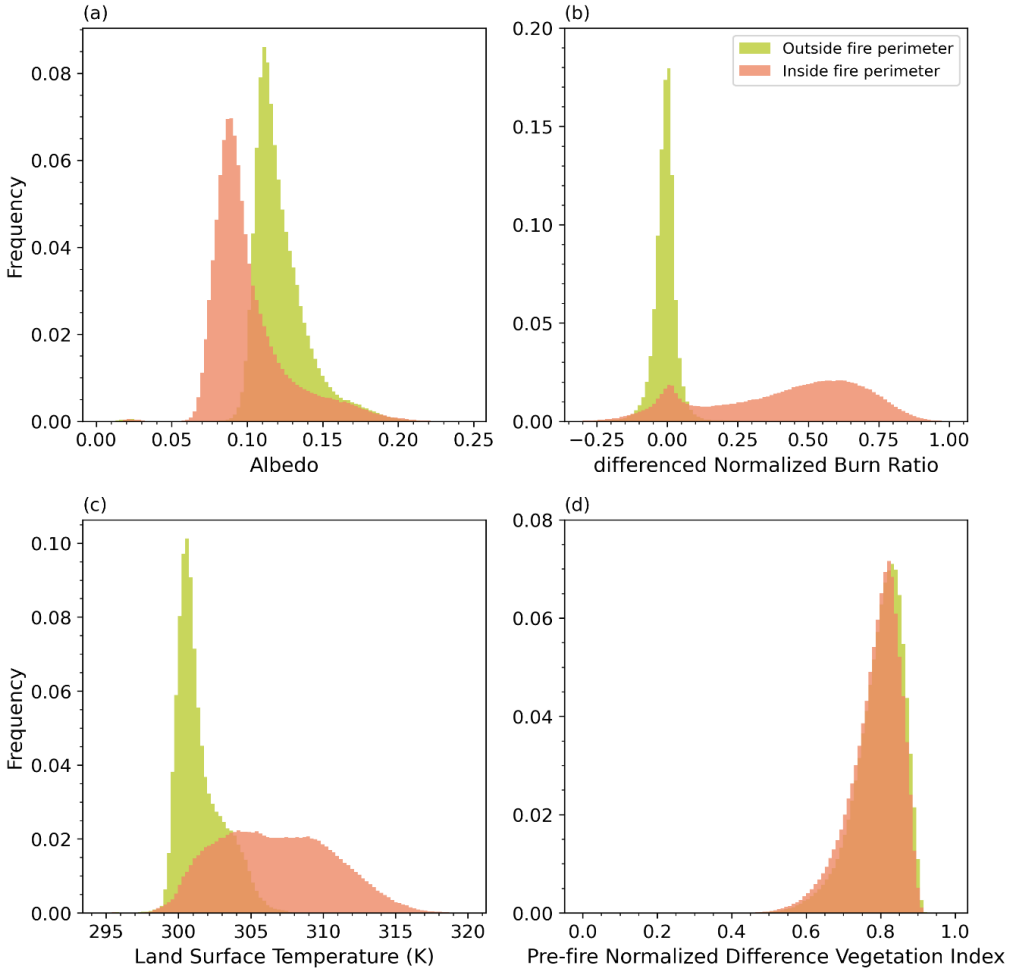

Figure R6: Relative frequency distributions of remote sensing proxies derived from Landsat 8 imagery inside and outside the fire perimeters:(a) albedo, (b) differenced Normalized Burn Ratio, (c) land surface temperature, and (d) pre-fire Normalized Difference Vegetation Index. The pixels outside the fire perimeter were within 2 km from the fire perimeter.

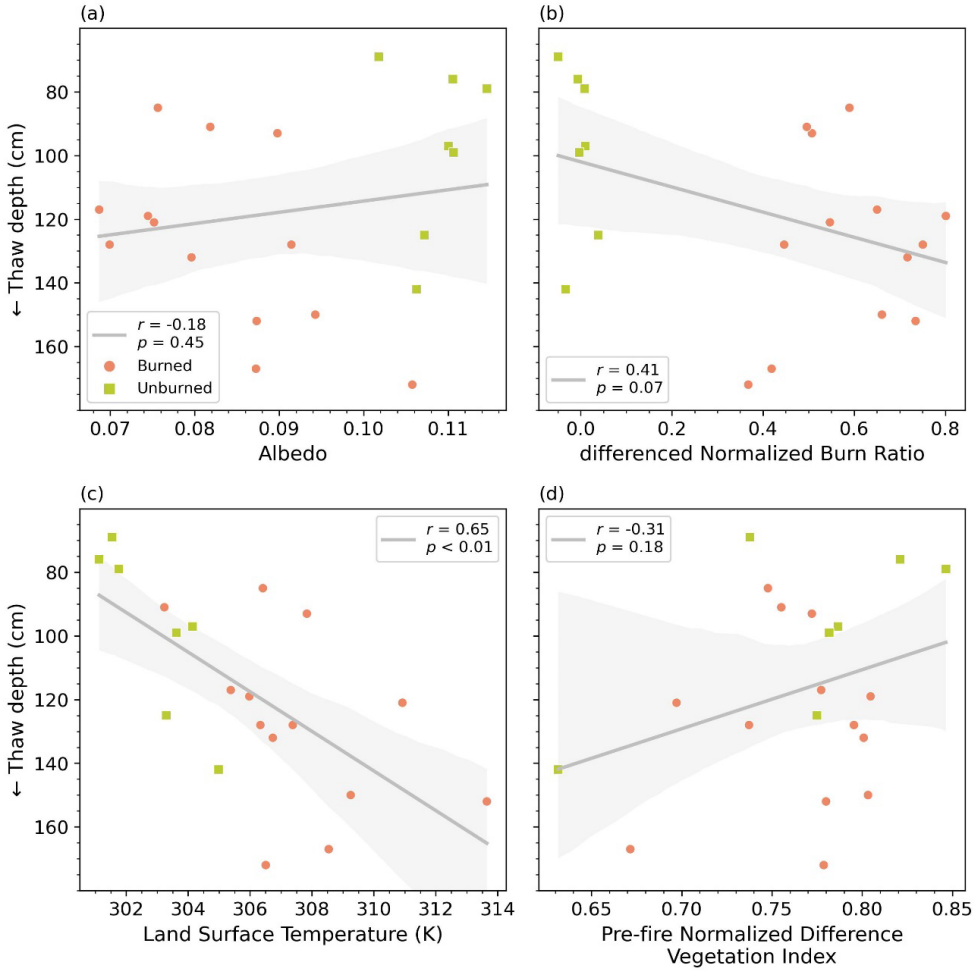

Figure R7: Scatter plots and linear regression lines between field-measured thaw depth and remotely sensed (a) albedo, (b) differenced Normalized Burn Ratio, (c) land surface temperature, (d) pre-fire Normalized Difference Vegetation Index.

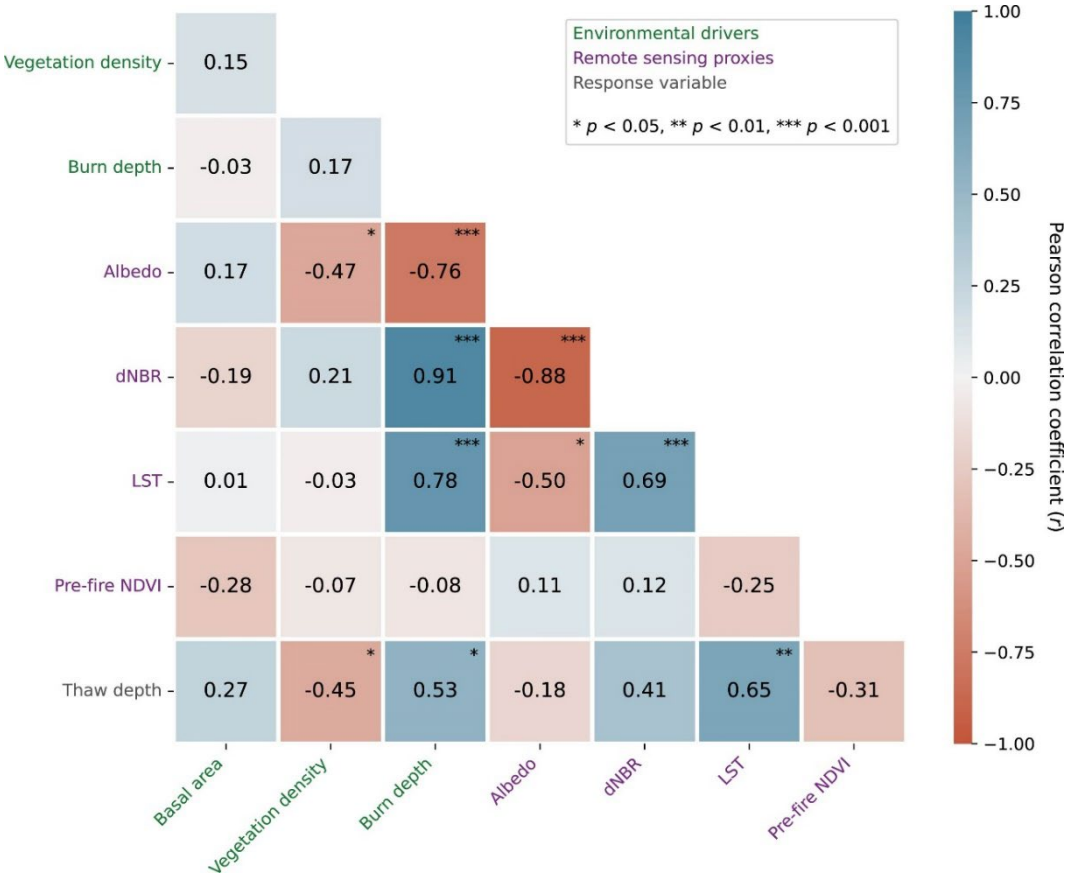

Figure R8: Correlation matrix of selected environmental drivers, remote sensing proxies, and thaw depth. GeoCBI is the Geometrically structured Composite Burn Index. LST is the land surface temperature. dNBR refers to the differenced Normalized Burn Ratio and NDVI to the Normalized Difference Vegetation Index.

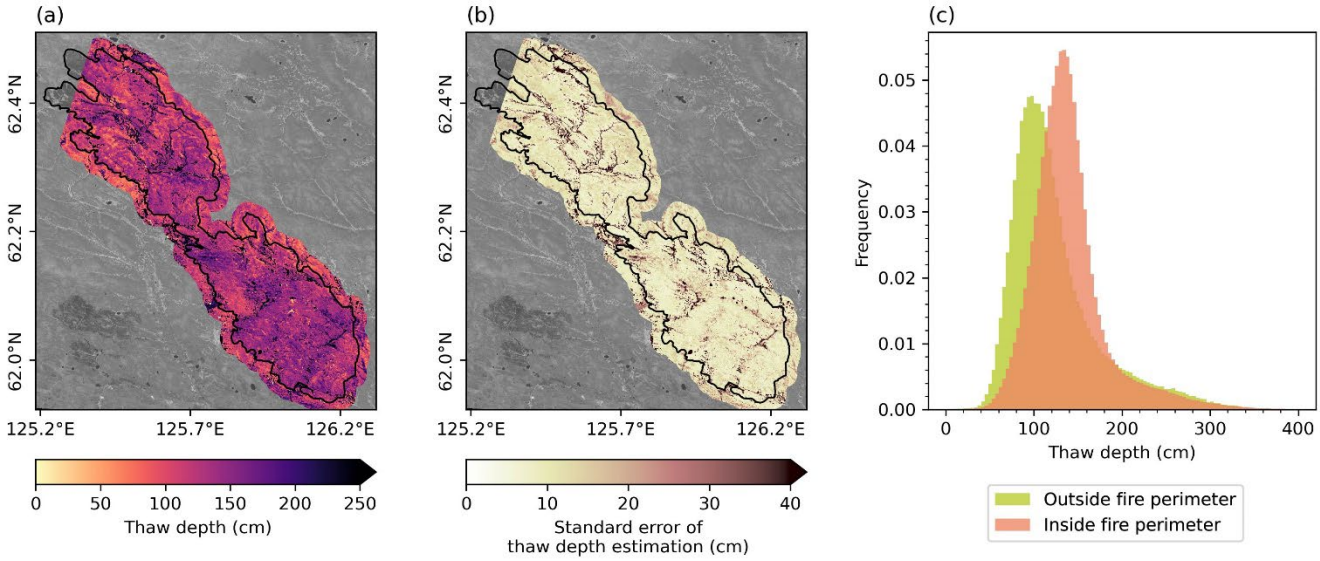

Figure R9: Maps of (a) estimated thaw depth, (b) its standard error, and the (c) relative frequency distribution for the pixels inside and outside the fire perimeter. The pixels outside the fire perimeter are within 2 km from the fire's edge.

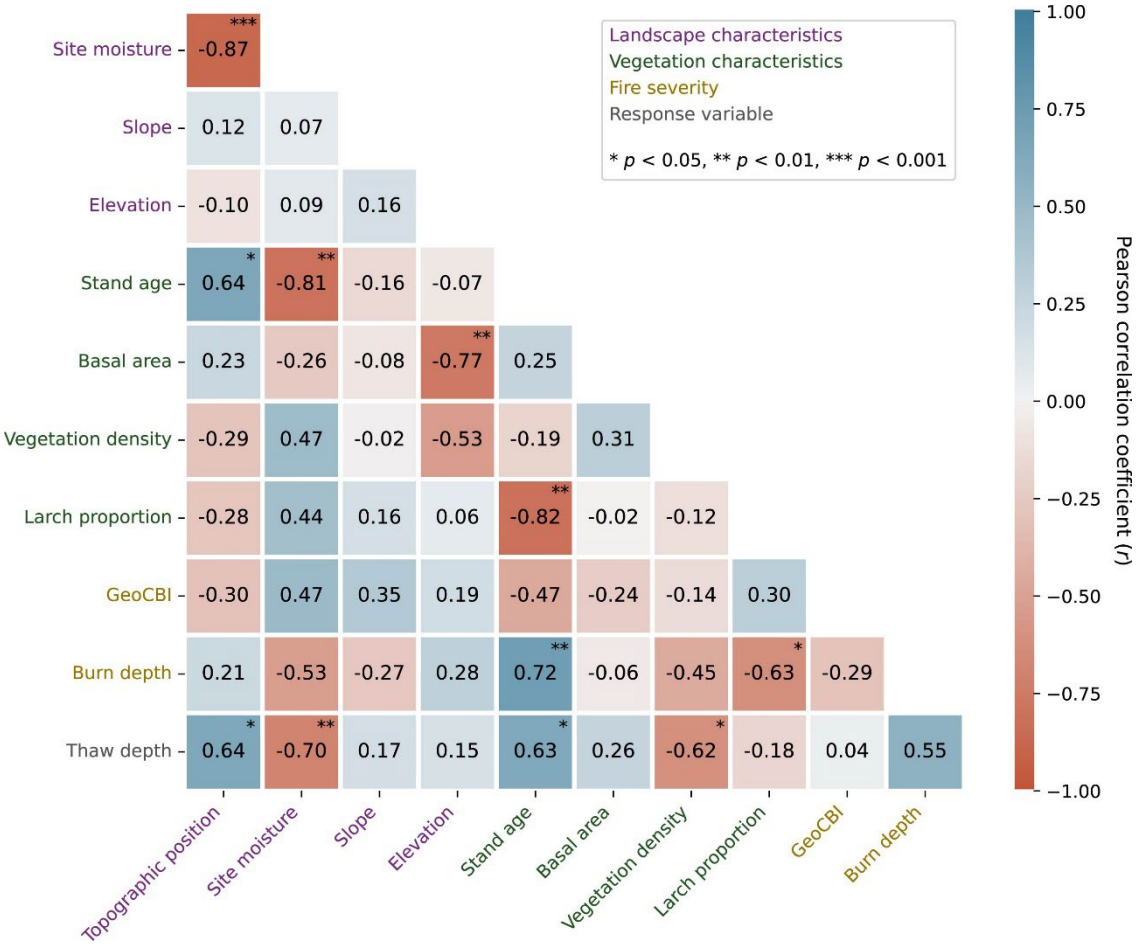

Figure R10. Correlation matrix between field-measured environmental variables representing landscape, vegetation and fire severity characteristics, and thaw depth, including only burned plots.

Table R1: Summary of the multiple linear regression for the environmental drivers of thaw depth. *SE* is the standard error of the corresponding variable's coefficient. The R^2 column displays the coefficient of determination of each predictor variable separately as well as for the multiple linear regression model. The relative importance indicates the contribution of each independent variable to the multiple linear regression model R^2.

Independent variables	Coefficient	*SE*	*t*	$p > \|t\|$	R^2	Relative importance (%)
Basal area	1.51	0.51	2.96	<0.001	0.07	14.7
Vegetation density	-10.47	2.24	-4.68	0.009	0.20	38.4
Burn depth	3.88	0.78	4.96	<0.001	0.28	46.9
Constant	82.36	13.32	6.18	<0.001		
Multiple linear regression model					0.73	

Table R2: Summary of the multiple linear regression for the remote sensing proxies of thaw depth. *SE* is the standard error of the corresponding variable's coefficient. The R^2 column displays the coefficient of determination of each predictor variable separately as well as for the multiple linear regression model. The relative importance indicates the contribution of each independent variable to the multiple linear regression model R^2.

Independent variables	Coefficient	*SE*	*t*	$p > \|t\|$	R^2	Relative importance (%)
Albedo	2807.88	674.09	4.16	0.001	0.03	24.0
differenced Normalized Burn Ratio	167.89	33.01	5.08	<0.001	0.17	47.7
Pre-fire Normalized Difference Vegetation Index	-399.24	97.12	-4.11	0.001	0.10	28.3
Constant	99.64	77.27	1.29	0.216		
Multiple linear regression model					0.66	